MONTHLY WEATHER REVIEW
VOLUME 97, NUMBER 5
MAY 1969

UDC 551.524.735:551.510.53:551.511.33:551.521.17:535.34

A SIMPLIFIED METHOD OF COMPUTING STRATOSPHERIC HEATING RATES AND ASSOCIATED GENERATION OF AVAILABLE POTENTIAL ENERGY

GASTON PAULIN [1]
Meteorological Service of Canada, Department of Transport, Montreal, Quebec

ABSTRACT

A method of computing the stratospheric heating rates from available daily data of the Northern Hemisphere is given. It consists of a hybrid approach using both the simple parametric equations in the solar ultraviolet absorption and the radiative transfer equations in the long-wave spectrum (15-micron carbon dioxide and 9.6-micron ozone absorptions). This method has been applied in the stratosphere for the period Jan. 12 to 16, 1959, in order to compute the generation of available potential energy. The results indicate that the method, as well as being suitable for energy budget studies over longer periods of time, is sufficiently accurate to enable one to describe synoptically some of the aspects of the radiative exchange between troposphere and stratosphere.

1. INTRODUCTION

Diagnostic studies of the atmosphere have been held up for a long time by the staggering problem involving the solution of the radiative transfer equations. Through the years many simplifications to these equations were formulated, and with the gradual increase of knowledge of the distribution of the absorbing gases, a climatology of radiative field distribution emerged. However, the computations of the daily variations of this heating field and ensuing generation of available potential energy were still very lengthy. Recently, to circumvent this direct approach, the daily generation of available potential energy was obtained indirectly from inconsistencies in adiabatic vertical motion computations as shown by Wiin-Nielsen (1964) and applied by Brown (1964), Muench (1965), Julian and Labitzke (1965), and Perry (1966). The present study, however, goes back to the radiative transfer problem and incorporates a shortcut method to evaluate the daily stratospheric heating rates directly from the corresponding semihemispheric temperature fields. The effect of large-scale cloud patterns on the stratospheric heating balance is included. The resulting heating rates are used to compute the generation of available potential energy in the stratosphere and its distribution in the vertical, in the wave number domain, and in time.

2. A DESCRIPTION OF THE METHOD

There have been many approximations developed for handling the radiative transfer problem. The author has done his best to go through these methods choosing those techniques that appear to give the most realistic results, bearing in mind that the method should be simple and readily applicable to available synoptic data. The following will describe the method finally chosen to handle the different radiative transfer components.

DATA

The original data consisted of the daily temperature fields at nine atmospheric levels (850, 700, 500, 300, 200, 100, 50, 25, and 10 mb) in the area from 30° N. to 80° N., for the period Jan. 12 to 16, 1959. Most of the data came from maps analyzed at McGill University, except that the 50- and 10-mb data were obtained from a series of maps published for the Free University of Berlin (Kreister et al., 1962; Labitzke-Behr et al., 1962). Large-scale cloud systems were also included to be used in the solution of the radiative transfer associated with the 9.6-micron band ozone absorption.

TOTAL SOLAR HEATING RATES

Hering et al. (1967) found a very strong correlation coefficient between solar heating rates (computed using the lengthy transfer equations) and a combination of solar zenith angle and sunlight duration. The proposed linear relation is the following:

$$(\partial T/\partial t)_s = an\overline{M}^{-1/2} + b \qquad (1)$$

where $(\partial T/\partial t)_s$ is the total solar heating rate in °C day $^{-1}$, n is the duration of sunlight in hours, $\overline{M}$ is the magnification of vertical path length for slant path transmission averaged over the daylight hours (Houghton, 1963), and a, b are the linear regression coefficients listed in table 1. As noted from this table, the correlation is best at 25 mb where the latitudinal variation of ozone is at a minimum, while differences at 15 mb and 10 mb, although small, are systematic and are due to the higher ozone concentrations

[1] Work done while on educational leave in the Department of Meteorology, McGill University, Montreal, Quebec.

near the Equator and lower concentration in the Arctic at these levels (Hering et al., 1967).

TABLE 1.—*Correlation coefficients r, standard error σ (°C day⁻¹), and linear regression constants a and b, for the relationship between $(\partial T/\partial t)_s$ in °C day⁻¹ and $n\overline{M}^{-1/2}$*

Pressure (mb)	r	σ	a	b
25	.990	.056	.142	.071
15	.972	.156	.230	.081
10	.971	.185	.272	−.109

Hering approximates the "$n\overline{M}^{-1/2}$" term by the relation

$$n\overline{M}^{-1/2}=A+B\cos(2\pi t/365) \quad (2)$$

where t is the number of days after the summer solstice, and the two constants A and B are given for 10° latitude intervals in table 2. The term "$n\overline{M}^{-1/2}$" is approximated within a few percent by (2). Since this study is concerned with latitude intervals of 5°, A and B values at the missing latitudes were interpolated from table 2.

This study combines (1), (2), and their associated tables 1 and 2 to compute total zonal solar heating in the appropriate period, i.e., January. The values vary slightly from day to day as n and $\overline{M}$ are functions of time, t.

The corresponding solar heating rates at 50 mb and 100 mb were taken from Kennedy's (1964) January cross-section. These heating rates resulted from energy transfer computations applied to the mean January ozone distribution derived from the ozonesonde reports. The heating rates due to absorption of near-infrared solar radiation were also taken from Kennedy (1964), whose methods were based on Houghton (1963) and whose temperature structure was that of a 3-yr-averaged cross section for January. Although this last approximation is cruder than the computation at 10 mb and 25 mb, it is validated by the fact that the heating rates are one order of magnitude or more smaller than those at upper levels due to the rapid exponential decrease in the solar radiative fluxes reaching those lower levels.

INFRARED TRANSFER DUE TO WATER VAPOR

The stratospheric heating rates due to water vapor in the infrared have been found to be relatively small compared to other stratospheric absorbing gases (Paulin, 1966; Kennedy, 1964; Davis, 1963). Representative magnitudes of the cooling rates associated with this radiative component would range from 0.3°C day⁻¹ at 100 mb to 0.1°C day⁻¹ at 10 mb. Further, Davis (1961) has shown that midtropospheric clouds have little effect on the water vapor radiative flux divergence in the stratosphere. According to these facts, the mean January zonal heating rates due to the water vapor computed by Kennedy (1964) were accepted at the stratospheric levels.

INFRARED TRANSFER DUE TO THE 15-MICRON BAND OF CARBON DIOXIDE

Rodgers and Walshaw (1966) found that the radiative cooling in the stratosphere can be approximated fairly accurately by the cooling-to-space component, which depends on the emitter temperature and the amount of absorber between the emitter and space. On the other hand, a relatively fast method of evaluating the carbon dioxide cooling rates was available from Kennedy's work. It had the advantage of incorporating both the cooling-to-space and the intermediate layer interaction components. Because of these, Kennedy's method was chosen, and it will be described in the next few paragraphs.

TABLE 2.—*Constants A and B of equation (2) as a function of latitude*

Latitude (° N.)	10	20	30	40	50	60	70	80
A	10.02	9.85	9.56	9.18	8.70	8.36	7.80	7.12
B	0.78	1.58	2.43	3.36	4.43	6.07	7.13	8.30

The usual constancy of CO_2 concentration is used. The fractional concentration by volume is assumed constant at 0.00031 (Kennedy, 1964; Ohring, 1958). The heating rate due to infrared transfer in a layer of thickness Δp is:

$$\partial T/\partial t=(g/c_p)\Delta F/\Delta p \quad (3)$$

where ΔF is the net upward flux over a layer Δp mb thick. The spectroscopic data used were those of Burch et al. (1962), as applied to the 12- to 18-micron interval. The black-body flux for this interval was computed from an expression presented by Davis (1961):

$$B(\text{cal/cm}^2\text{ min})=116.435-1.6704T+0.0063T^2\times10^{-3}, \quad (4)$$

where T is the mean temperature of the layer. Kennedy rearranged (3) into the form:

$$(\partial T/\partial t)\,(°\text{K/day})=(gA/c_p)\sum_{i=1}^{31}(\Delta B_i\Delta a_i)/\Delta p \quad (5)$$

where Δa_i is the difference in absorptivities in layer i, ΔB_i is the difference in black-body flux in the same layer, and A is a conversion constant. Incidentally, when ΔB_i is in cal cm⁻² min⁻¹, Δp is in millibars and $\partial T/\partial t$ is in °K day⁻¹, the constant gA/c_p is 5889.6. Kennedy gives a table for sets of 31 ΔB_i and Δa_i values corresponding to 14 stratospheric layers extending from 200 mb to 5 mb. The heating rates can be found at these 14 layers. The computations require temperatures at 31 atmospheric layers—from surface to 0.6 mb. Kennedy shows that the atmospheric structure below midtroposphere contributes little to the stratospheric heating rates. The effect of cloudiness below 500 mb will be negligible in the stratosphere, and in the present computations the 500-mb temperatures are chosen to be those of the lower boundary. This speeds up the computations by a factor of 1.5; that is, only 21 layers are required instead of 31. The temperatures needed at Kennedy's level were interpolated from the hemispheric data at 500 mb, 300 mb, 200 mb, 100 mb, 50 mb, 10 mb, and 2 mb. The heating rates were computed at every grid point separated by 5° latitude and 10° longitude from 30° N. to 80° N. for the period of Jan. 12 to 16, 1959. The heating at the levels given above is interpolated again from the results.

INFRARED TRANSFER DUE TO OZONE IN THE 9.6-MICRON BAND

The infrared radiative transfer method for the 9.6-micron band of ozone used by Paulin (1966) will be described and applied to the data.

The atmosphere is transparent to black-body radiation emitted in the spectral region between about 8 and 13 microns. This "window" coincides fairly well with the maximum black-body emission of terrestrial radiation. There is an ozone absorption band centered at 9.6 microns. Since the ozone amount in the troposphere is very small, the upcoming flux through this atmospheric window will be effectively absorbed by the much higher amount of ozone in the lower stratosphere where significant heating rates will presumably follow. Of particular interest is the temperature fluctuation of the lower boundary which is assumed to be a black body. Paulin (1966), Kennedy (1964), and Clark (1963) have all computed the heating changes following a variable lower boundary temperature. The presence of thick middle clouds will then modulate the stratospheric heating rates. Because of latitudinal characteristics of both the temperature and the ozone vertical profiles in winter, the influence of the lower emitter becomes insignificant north of 50° N., relaxing the requirement of clouds north of this latitude.

The atmosphere was divided into 18 quasi-equal layers, except that the troposphere (defined as the portion of the atmosphere lying below 314 mb) was chosen as the lowest layer, since the amount of ozone in this layer is comparable to the amounts in the layers above. The ground or the cloud tops (for overcast conditions) were assumed to be black bodies while the top of the atmosphere was taken to be at 0°K. Paulin (1966) has shown that the net upward flux at level Z_i, $F_{net}(Z_i)$ may be expanded into a matrix product of the form:

$$\begin{Bmatrix} F_{net}(Z_1) \\ F_{net}(Z_2) \\ F_{net}(Z_4) \\ \vdots \\ F_{net}(Z_{18}) \\ F_{net}(Z_{19}) \end{Bmatrix} = \begin{Bmatrix} 2A_r(1,1) & A_r(1,2) & A_r(1,4) & \cdots & A_r(1,18) & A_r(1,19) \\ A_r(2,1) & A_r(2,2) & A_r(2,4) & \cdots & A_r(2,18) & A_r(2,19) \\ A_r(4,1) & A_r(4,2) & A_r(4,4) & \cdots & A_r(4,18) & A_r(4,19) \\ & & & & & \\ A_r(18,1) & A_r(18,2) & A_r(18,4) & \cdots & A_r(18,18) & A_r(18,19) \\ A_r(19,1) & A_r(19,2) & A_r(19,4) & \cdots & A_r(19,18) & A_r(19,19) \end{Bmatrix} \times \begin{Bmatrix} \overline{B(Z_1)}-0 \\ \overline{B(Z_3)}-\overline{B(Z_1)} \\ \overline{B(Z_5)}-\overline{B(Z_3)} \\ \vdots \\ \overline{B(Z_{19})}-\overline{B(Z_{17})} \\ 0-\overline{B(Z_{19})} \end{Bmatrix} \quad (6)$$

where $A_r(i,j)$ is the 9.6-micron ozone band absorptivity (the original spectral data were taken from Walshaw, 1957) from level Z_i to level Z_j, while $B(Z_m)$ refers to the black-body flux at the temperature of level Z_m. In the present spectral region, (3) becomes:

$$(\partial T/\partial t)(^\circ\text{K day}^{-1}) = 35.3376 \times 10^4[F_{net}(Z_{i+2}) - F_{net}(Z_i)]/(p_{i+2} - p_i) \quad (7)$$

when F_{net} is in cal sec^{-1} cm^{-2} and p is in millibars.

It was considered useful to approximate the effect of cloudiness on the heating rates in the stratosphere. The problem becomes one of incorporating (7) into our data.

First, one must define a hemispheric ozone distribution representative of the month of January. Dutsch (1964) has presented seasonal vertical ozone distributions over selected latitudes, based on the Umkehr method. Bojkov (1965) has also presented ozone vertical profiles over the world based on both the Umkehr method (3,700) and on ozonesonde reports (about 200). Because of the much greater number in the former cases, the statistics will be normally biased toward the Umkehr determinations. There has been some criticism of the Umkehr method; Mateer's (1964) study of the Umkehr method has shown its limitations as far as the number of independent pieces of information is concerned, and inferences from specific profiles (Bojkov, 1966) confirmed the difficulties encountered in comparing the two methods. On the other hand, Kennedy (1964) has computed average ozone cross-sections based on January–February 1963 ozonesonde reports over North America. Hering and Borden (1965) have abstracted mean seasonal cross-sections from the 2-yr period 1963–64. Although these observations were mostly over North America and far less numerous than the compiled Umkehr determinations, it is felt that the ozonesonde reports and statistics would be more representative and physically more acceptable. Following these arguments, the winter mean cross-sections as given by Hering and Borden (1965) were adopted as representative of hemispheric distributions.

As indicated earlier, the temperature at the lower boundary has a one-to-one correspondence to the heating encountered in the lower stratosphere. This study is biased toward a large-scale resolution. The next logical step is to define the synoptic cloud patterns over our region. Their spatial distribution will define a variable radiant flux emanating from the tropospheric lower boundary via the 9.6-micron absorption band. This energy flux will be modified further by the vertical ozone profile. The southernmost ozone profile has its maximum concentration at a higher altitude, is more sharply defined,

TABLE 3.—*Heating rate (°C day^{-1}) due to the absorption of terrestrial radiation by the 9.6-micron band with variable lower boundaries*

Latitude	30° N.	50° N.	70° N.
Clear conditions	0.56	0.20	0.04
Overcast tops at 500 mb	0.24	0.14	0.03
Overcast tops at 300 mb	0.10	0.05	0.03

and shows a larger concentration; whereas the Arctic profile is broader and has a lower concentration at its level of maximum concentration. From this it follows that the magnitude of the heating will decrease with latitude for a similar temperature profile. In addition, the temperature structures of the southern and the northern regions in winter are quite different. The temperature difference between the lower boundary and the level of maximum heating is much larger in the southern regions. The amplitude of the radiant flux variations associated with the clear-to-cloudy intersections becomes of the order of the error in computing heating rates over the northern regions. Table 3 shows an example of computation at various latitudes using our selected ozone profile. In view of the results from table 3, it was decided to omit the cloud effects for the regions north of 50° N. For the regions bounded by 30° N. and 50° N., one of the lower boundary temperatures (850 mb and 500 mb) was accepted, 850 mb being the lowest temperature level available in this study. This can be taken as a very conservative level since it approximates the temperature of the low cloud tops, on the nonsynoptic scale, especially applicable over oceanic areas.[2] The 500-mb temperature was chosen in case of a synoptic cloud cover. This is a conservative estimate of the highest clouds behaving as black bodies. The next step was to define the cloud patterns from the available data. The decision to call a region cloudy or not was based on three different tests. At 500 mb, areas of dew-point depression less than or equal to 2°C were contoured. Areas of observed overcast conditions were also defined. Thirdly, areas of positive vorticity advection were also determined. Finally, the intersection of these areas was formally called overcast with tops at 500 mb.

The vertical temperature structure of each grid point was interpolated to fit the radiative model. The resulting heating rates were re-interpolated at the four stratospheric mandatory levels of 100 mb, 50 mb, 25 mb, and 10 mb for each grid point and for the 5 days included in the period Jan. 12 to 16, 1959. It was thought that in following those rules, the signal received in the stratosphere from the troposphere in the 9.6-micron band would be appropriately defined—even if the amplitudes were somewhat conservative, the phase of the signal should be relatively accurate. These mean zonal heating rates due to the 9.6-micron band are on the average a bit less than those computed by Kennedy. This is due mainly to three causes. The use of pressure scaling by Kennedy versus the Curtis-Godson approximation used in the present study will cause some change in the results. Probably more important systematic effects are the inclusion of clouds in our model, which decrease the mean zonal heating, and the systematic use of the 850-mb temperature as the emitting lower boundary. Smaller differences may also be due to the layering system in the model and to the difference between the real temperature fields against a climatological mean temperature.

[2] The radiant flux assigned to the sunny and snow-free land areas is necessarily underestimated in this study.

3. THE TOTAL HEATING FIELDS

The components of the heating field were added together and gave the total field due to the absorption of solar and terrestrial radiation at 10, 25, 50, and 100 mb over the chosen 5-day period. The eddy heating fields were generated by the infrared transfer due to the stratospheric absorption by the 9.6-micron band of ozone and by the 15-micron band of carbon dioxide. The zonal heating configurations were given by the solar ultraviolet absorption and the zonal part of the infrared absorption mentioned above.

The semihemispheric temperatures and heating rates for Jan. 12, 1959, may be seen on figures 1 to 4. The relative similarity of the heating curves with the temperature curves is evident and reflects, in a large part, the strong influence of the Newtonian cooling component of the 15-micron band of carbon dioxide. The effects of the clouds (at and south of 50° N.) on the total radiative heating rates at 50 mb may be inspected from figure 5. This level was chosen because it is most sensitive to the temperature fluctuations of the lower boundary when the latter is assumed to act as a black body. The clouds are found to accentuate the total cooling rates, indicating a decrease in the absorption of the 9.6-micron band of ozone, and hence causing some radiative tropospheric-stratospheric interactions.

4. GENERATION OF AVAILABLE POTENTIAL ENERGY

Following Lorenz (1955), the generation of available potential energy G may be approximated by the heating rate-potential temperature covariance on an isobaric surface. More specifically the relation is:

$$G=(1/\Delta p)\int_{p_2}^{p_1}(S/c_p)(p_0/p)^{R/c_p}(h\theta)dp/g \qquad (8)$$

where p_1, p_2 are the layer-bounding isobaric surfaces whose difference is Δp, R is the dry air gas constant, c_p is the specific heat of dry air at constant pressure, h is the heating rate, θ is the potential temperature, and S is a stability term given by:

$$S=-(p/p_0)^{R/c_p}(R/p)(\partial\{\overline{\theta}^{\lambda}\}^{\phi}/\partial p)^{-1} \qquad (9)$$

where $\overline{(\quad)}^{\lambda}$ is the zonal latitudinal average and $\{\quad\}^{\phi}$ is the meridional average. In both averaging operators, λ and ϕ stand for the longitude and the latitude, respectively. Equation (8) may be partitioned into its zonal (GZ), eddy (GE), and spectral ($GE(n)$) forms by standard Fourier transformations.

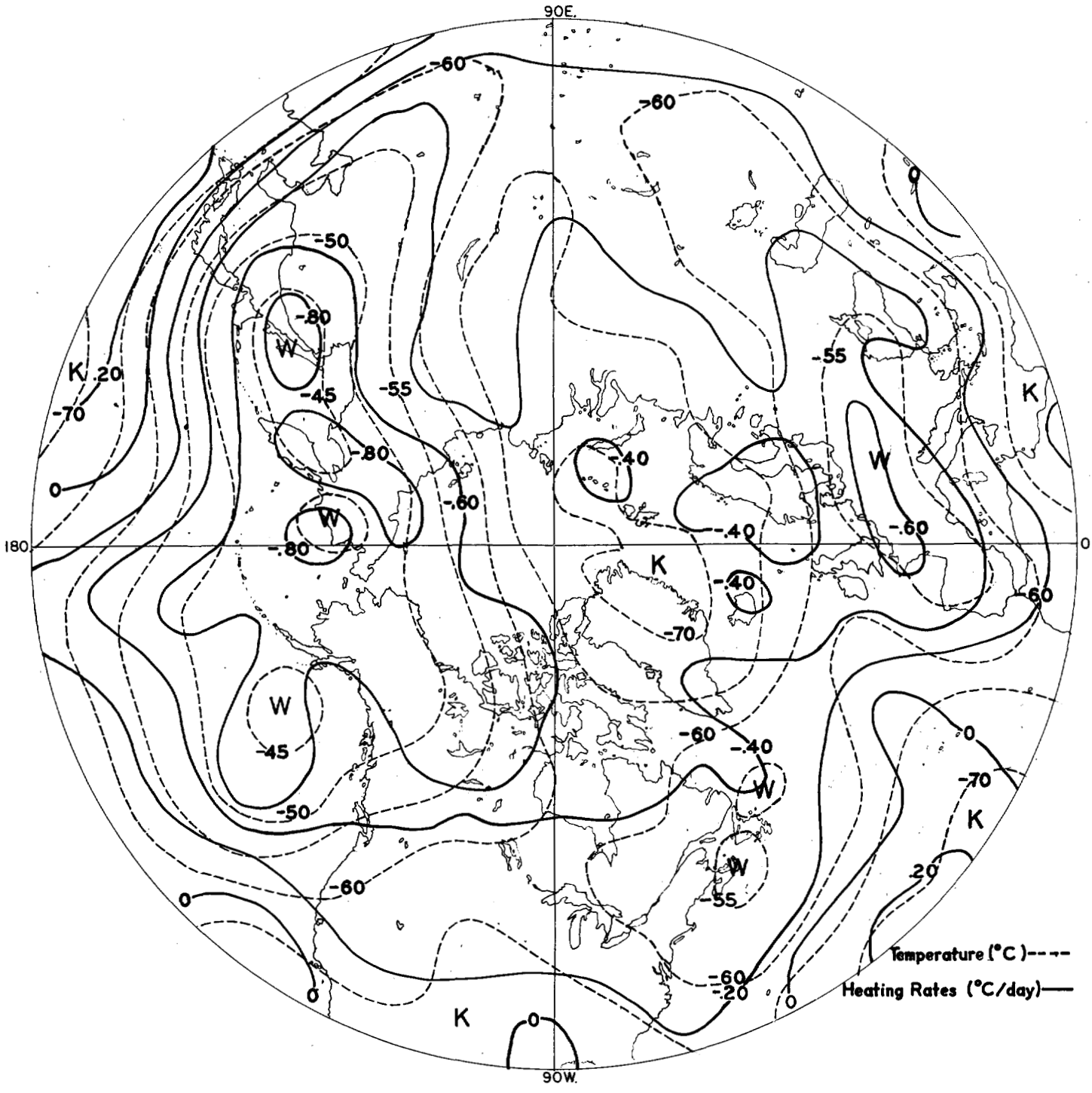

FIGURE 1.—Heating rates (°C day^{-1}) and temperatures (°C) at 100 mb on Jan. 12, 1959.

SOME SYNOPTIC RESULTS

The generation of available potential energy as applied to the whole stratosphere may be seen in table 4. GZ has small amplitude, decreases with time, and shows a slight positive time-averaged value. The total eddy (GE) and spectral ($GE(n)$) terms are uniformly negative and randomly variable in time. The spectral $GE(n)$ processes decrease in importance with increasing wave numbers. More information may be gained through the vertical distribution of these processes at the four stratospheric levels of 100, 50, 25, and 10 mb. Table 5 lists the zonal generation of available potential energy at those levels for the chosen time period. The positive GZ values at 25 and 10 mb show that a larger amount of insolation is absorbed at the latitudes where the mean zonal temperature is larger, and vice versa. Note that the effect of the zonal solar absorption surpasses the effect of the zonal cooling of the Newtonian type at these altitudes. The 100-mb generations are uniformly negative and reflect the preponderance of the Newtonian cooling. The 50-mb monotonic decrease of GZ in time may be related to a gradual and systematic cooling near 50 mb and at the

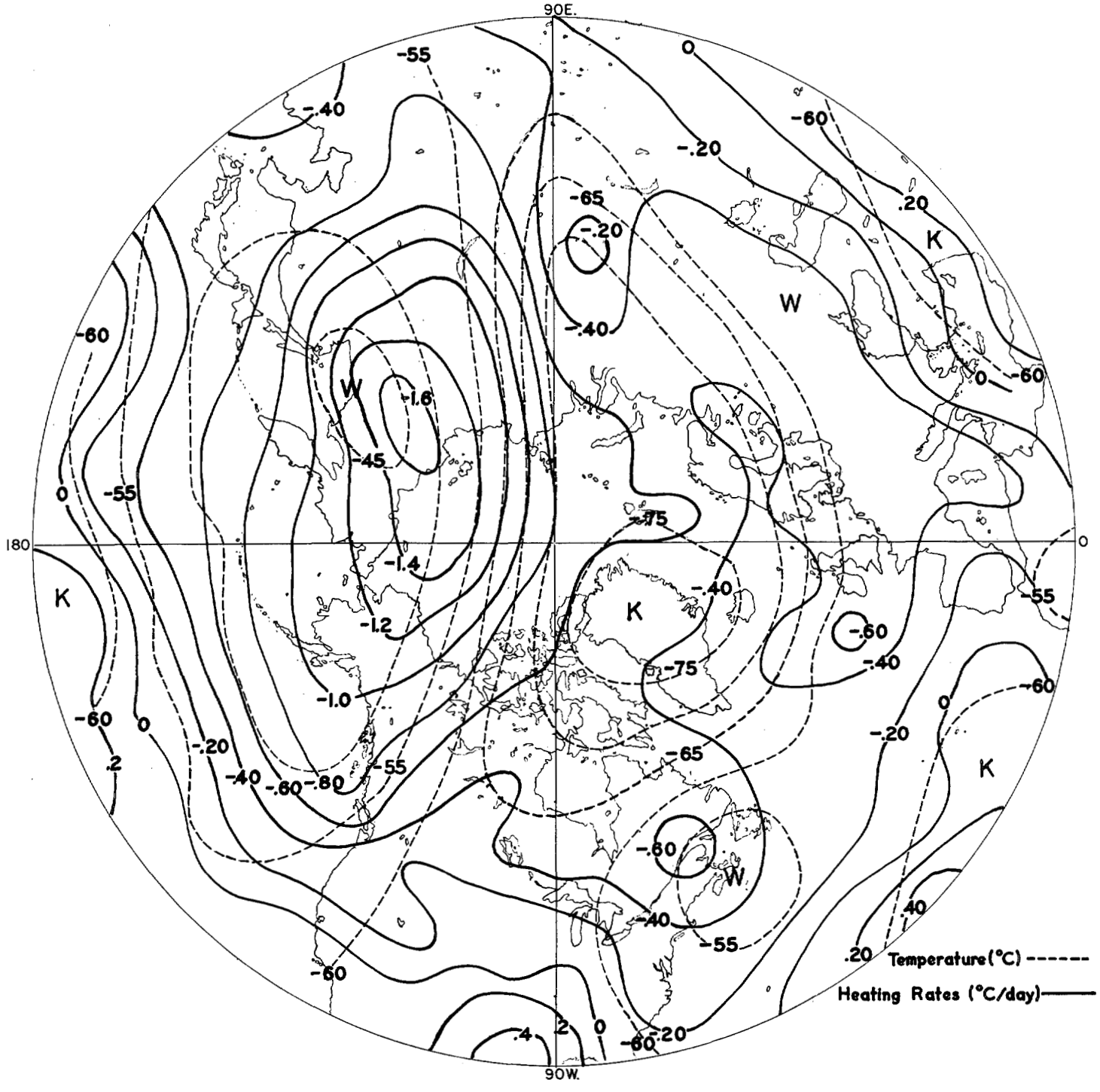

FIGURE 2.—Heating rates (°C day^{-1}) and temperatures (°C) at 50 mb on Jan. 12, 1959.

lower latitudes (30° N. to 45° N.); this was taken from the daily zonal temperature profiles in the vertical (not shown here). This change in the curvature at 50 mb favors a decrease in the carbon dioxide cooling over relatively colder regions and contributes to a decreasing zonal generation of available potential energy in time at 50 mb.

In a spectral energy study, Paulin (1968) found that some of the unbalance of the eddy available potential energy budget could be caused in part by a systematic underestimation of the carbon dioxide cooling, due to a necessarily smooth vertical temperature profile. Further the lack of longitudinal detail in the ozone distribution affecting both short-wave and long-wave radiative solutions also led to a greater indeterminateness in the heating rates, although of lesser consequence than in the CO_2 case above. Notwithstanding these limitations, the vertical distribution of the spectral and eddy generations of available potential energy is exhibited in table 6. The negative eddy generations at 50 and 25 mb appear to be out of step when compared to values above and below. Further, this apparent anomaly is centered mainly in wave number 1

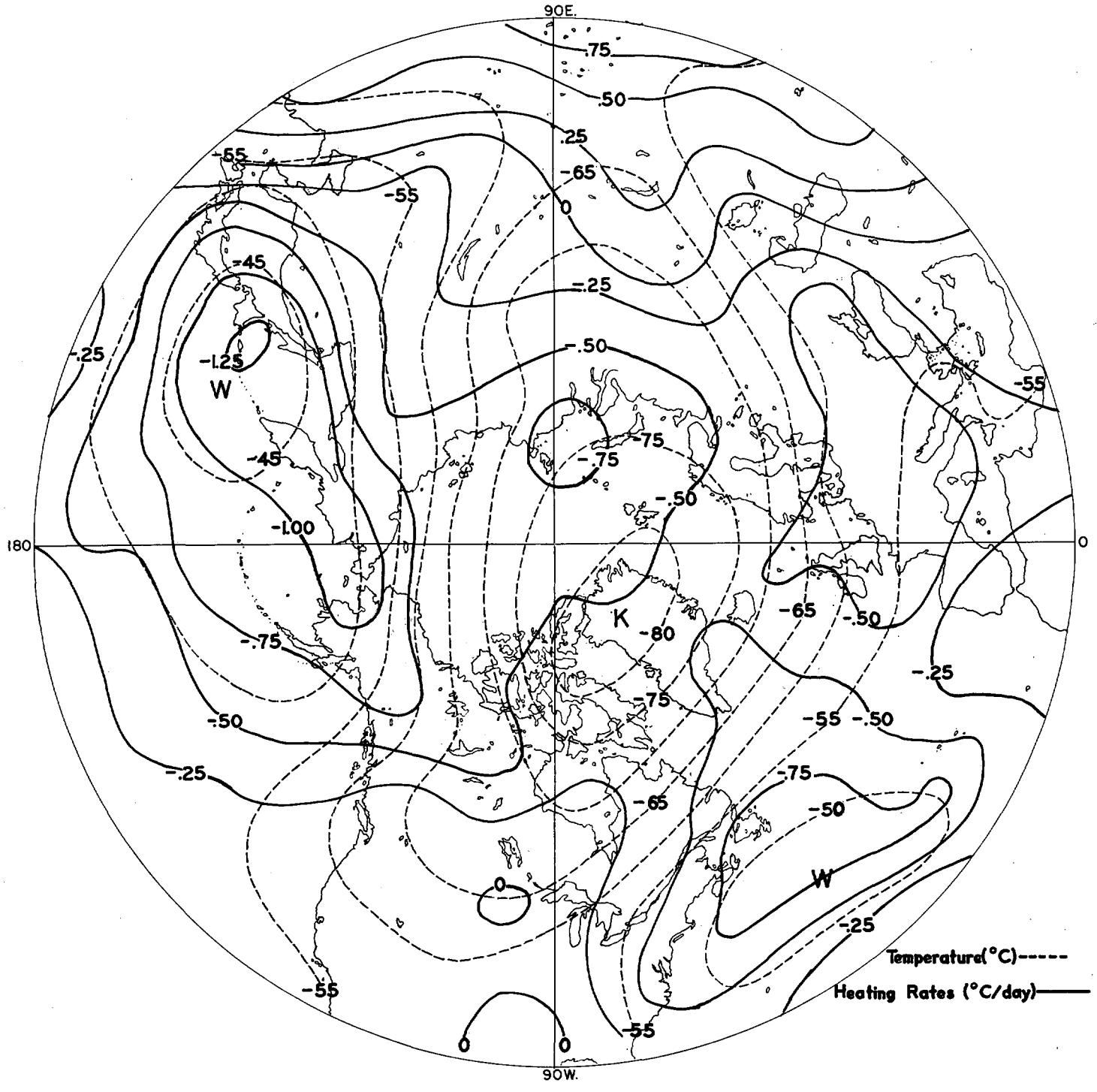

FIGURE 3.—Heating rates (°C day^{-1}) and temperatures (°C) at 25 mb on Jan. 12, 1959.

spatial generation. It is recalled that the generation formula (8) is modified by the stability parameter S, which is directly proportional to $(\partial\{\bar{\theta}^{\lambda}\}^{\phi}/\partial p)^{-1}$. It is found that this term tends to decrease the magnitude of the 25-mb generations when compared to those at 50 mb; whereas the 100-mb generation remains unchanged relative to the one at 50 mb. The predominance of wave number 1 at 50 mb is found to be produced by the latitudinal distribution of the covariance between the heating rates and the temperatures over the areas north of 45° N. The wave number 1 covariances at those latitudes and at 50 mb are five to 10 times larger than the corresponding wave number 2 covariances; whereas at 25 mb, both generation scales are found to be of the same order of magnitude.

Some interlevel radiative couplings are included implicitly in our computations via the carbon dioxide radiative transfer. Kinks in the vertical temperature profiles such as shown at 25 and 50 mb in figure 6 are smoothed radiatively, one kink feeding the other. It may be concluded that at both the 25- and the 50-mb levels, the large wave number 1 amplitude of the warm anticyclones over the northern regions combines to strengthen the

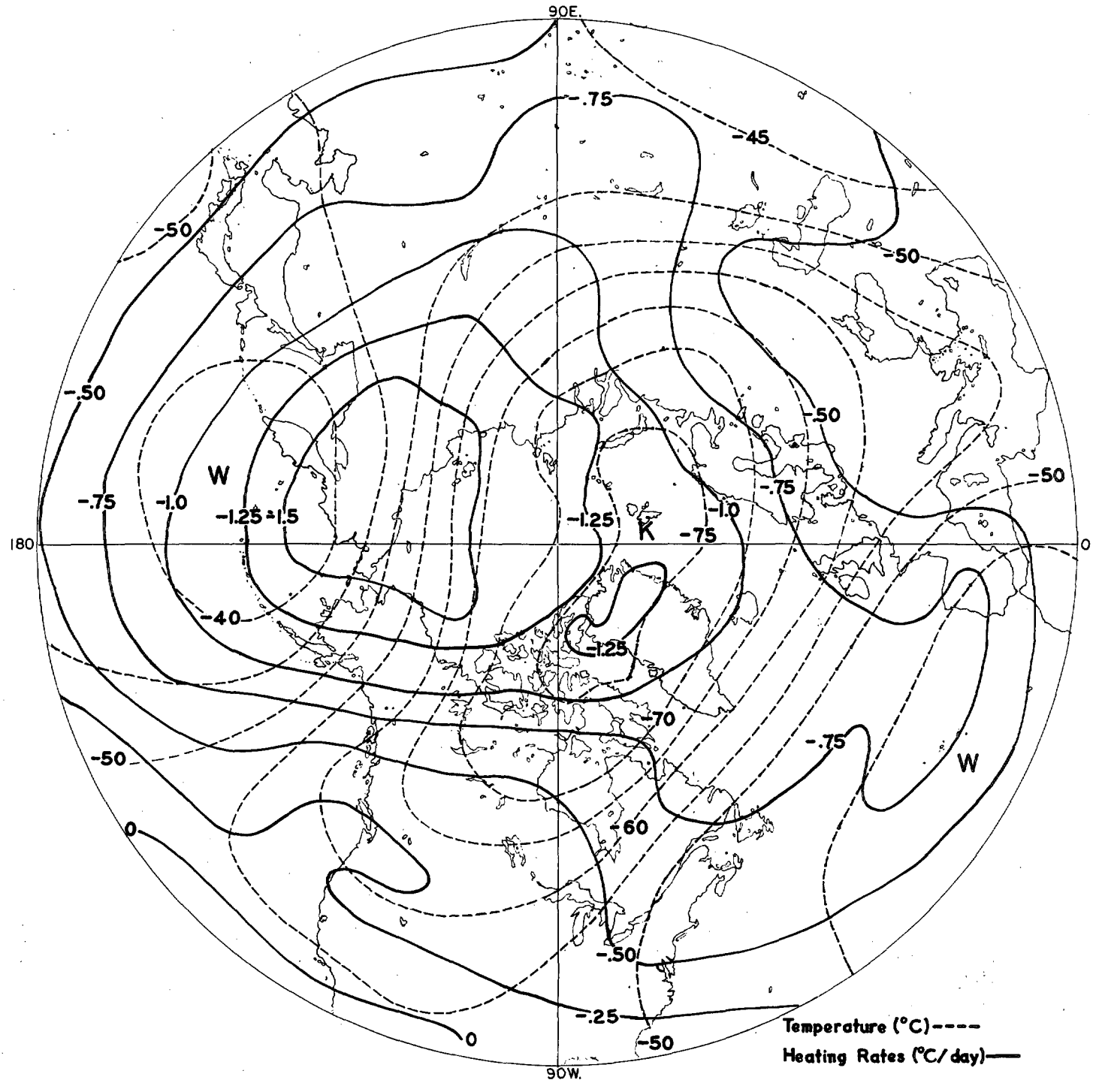

FIGURE 4.—Heating rates (°C day^{-1}) and temperatures (°C) at 10 mb on Jan. 12, 1959.

negative wave number 1 generation at 50 mb and to weaken the negative generation of the same scale at 25 mb.

Hence the anomaly in the vertical profile of the generation of eddy available energy has been analyzed and explained diagnostically by a stability effect and characterized by the predominance of the 50-mb heating rate field at wave number 1. It is presumed that the sink of eddy available energy at the scale of wave number 1 is accentuated at 50 mb and diminished at 25 mb via the carbon dioxide radiative transfer. It is then advanced that given a marked eccentric circulation at 25 and 50 mb (as is the case in our period), this radiative effect would cause persistent radiative interlevel couplings.

The tropospheric-stratospheric interaction via the absorption of terrestrial radiation in the 9.6-micron band of ozone is now considered. The lower boundary was chosen as the 850-mb level for clear skies and the 500-mb level for cloudy conditions. This lower boundary, by its characteristic temperature, has a strong influence on the ensuing heating rates in the 50-mb region. A latitudinal phase diagram pairing both temperature and heating rate

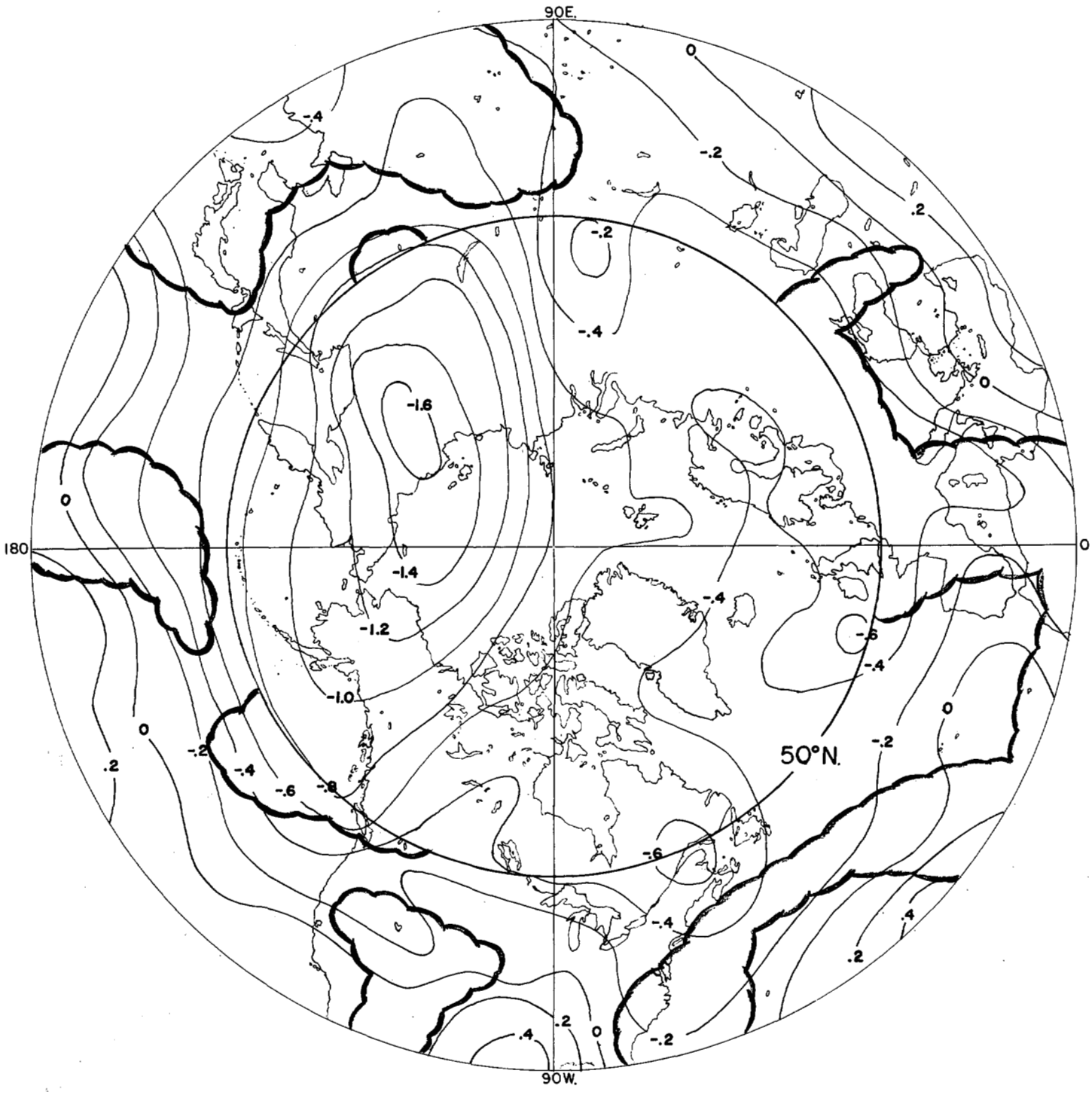

FIGURE 5.—Heating rates (°C day^{-1}) at 50 mb and large-scale cloud distribution between 50° N. and 30° N. on Jan. 12, 1959.

components due to the 9.6-micron absorption band for wave numbers 1 and 2, at 50 mb and 25 mb on Jan. 12, 1959, has been drawn as figure 7. A common characteristic emerges from the pairing—all correlations at all latitudes for both waves 1 and 2 are negative leading to an overall sink of eddy available energy. Negative heating rates prevail north of 35° N. and at 25 mb, since the maximum in the ozone density profile usually lies at or below this level and Newtonian cooling of the ozone at this level would contribute to a net negative generation. Wave number 2 emerges as the largest spectral contributor of the negative eddy generation of available energy at 25 mb. The radiative problem of the 50-mb level is quite different. Lying below the level of the maximum in the ozone vertical profile, positive heating rates would be encountered, modulated by the temperatures of the lower boundary. This heating leads again to a negative generation process, as shown by the negative correlation of the pairs at 50 mb on figure 7. The correlations at wave number 2 yield larger negative values than those of wave number 1. Inspection of the heating rates at the scales of wave numbers 3 and 4 yields values of the order of those

TABLE 4.—*Vertically integrated (100 mb to 10 mb) zonal and spectral generation of available potential energy for the period Jan. 12–16, 1959 (units: ergs cm^{-2} mb^{-1} sec^{-1})*

January 1959	12	13	14	15	16	Mean
GZ	.19	.08	−.00	−.00	−.06	.04
GE	−.82	−.89	−.91	−.91	−.92	−.89
GE(1)	−.45	−.51	−.49	−.47	−.51	−.49
GE(2)	−.20	−.20	−.26	−.23	−.22	−.22
GE(3)	−.05	−.06	−.05	−.08	−.09	−.07

TABLE 5.—*Daily and 5-day mean generation of zonal available potential energy GZ at individual stratospheric levels for Jan. 12–16, 1959 (units: ergs cm^{-2} mb^{-1} sec^{-1})*

January 1959	Level (mb)			
	10	25	50	100
12	1.90	.29	.41	−.35
13	1.74	.35	.16	−.41
14	1.53	.30	−.07	−.40
15	1.55	.24	−.09	−.16
16	1.53	.29	−.16	−.47
Mean	1.65	.29	.05	−.40

TABLE 6.—*Vertical distribution of the generation of eddy and spectral available potential energy in the stratosphere for Jan. 12 to 16, 1959 (units: ergs cm^{-2} mb^{-1} sec^{-1})*

Jan. 1959	Level (mb)	*GE*	*GE*(1)	*GE*(2)
12	10	−1.49	−0.70	−0.52
	25	−0.61	−0.18	−0.34
	50	−1.43	−1.01	−0.19
	100	−0.41	−0.18	−0.09
13	10	−1.68	−0.55	−0.87
	25	−0.77	−0.32	−0.35
	50	−1.44	−1.16	−0.11
	100	−0.47	−0.22	−0.04
14	10	−1.86	−0.45	−1.22
	25	−0.75	−0.41	−0.28
	50	−1.55	−1.05	−0.21
	100	−0.40	−0.24	−0.05
15	10	−2.19	−0.77	−0.98
	25	−0.86	−0.52	−0.22
	50	−1.26	−0.79	−0.26
	100	−0.45	−0.22	−0.04
16	10	−1.67	−0.68	−0.78
	25	−0.70	−0.39	−0.20
	50	−1.43	−0.99	−0.20
	100	−0.55	−0.26	−0.10

in wave numbers 1 and 2, but the temperature vectors are much smaller than those in the first two wave numbers, and further, their phase differences are much more randomly distributed, leading to an insignificant contribution to the generation of eddy available energy. The radiative signals at 50 mb generated by the lower boundary via the 9.6-micron band of ozone contribute about 15 percent to the negative generation of eddy available energy in wave number 1 and about 20 percent in wave number 2. These two waves, it is recalled, explain most of the eddy generation process.

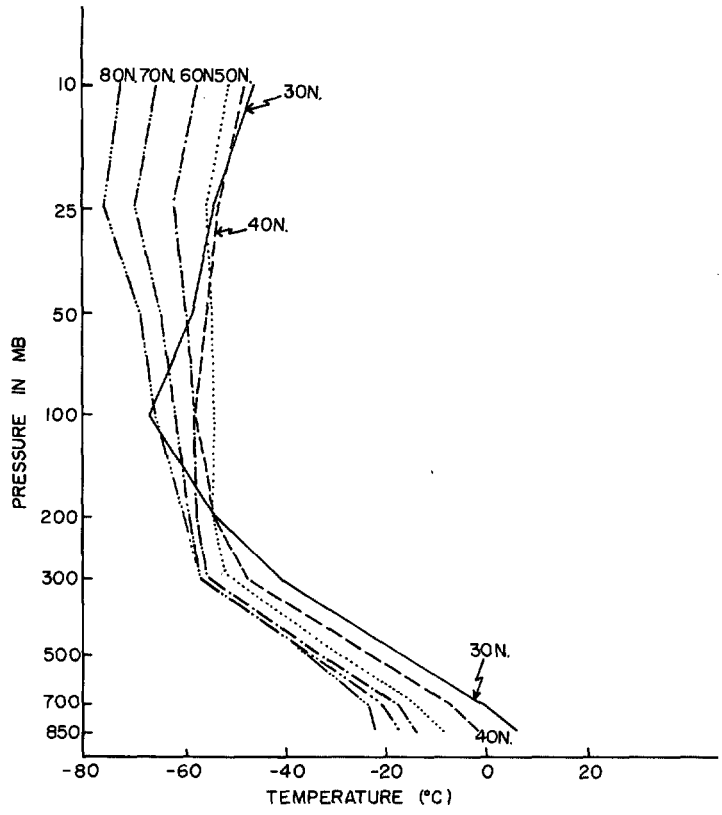

FIGURE 6.—Vertical profiles of the mean zonal temperatures at various latitudes in January 1959.

The synoptic patterns leading to the above results will now be described. A strong warm Aleutian high-pressure area and a weaker Atlantic anticylcone are found above the highly perturbed and cyclonically active regions in the troposphere. The extensive cloud area formed by the upward vertical motion (especially over the northern Pacific Ocean) is counteracted by the downward vertical motion aloft. The locally cold cloud tops reduce the heating influence of the net radiative (9.6 micron) flux convergence in the horizontally warmer regions of the 50-mb level. On the other hand, larger heating is found in the clear sky areas, corresponding to the horizontally colder 50-mb regions. Consequently, some of the existing eddy available potential energy is being destroyed. In a similar fashion, since the Aleutian High happens to be a wave number 1 or eccentric phenomenon, reinforced by wave number 2, the heating rate signals originating in the large-scale lower boundary temperature variations systematically destroy the existing available eddy energy at 50 mb.

COMPARISONS WITH OTHER STUDIES

The generations presented in this report are now compared with some other results found in the literature. Table 7 summarizes the results and their domains of applications. Most winter studies yielded rather small stratospheric zonal generations of either sign although Julian and Labitzke (1965) and Kennedy (1964) computed somewhat larger negative generations. The 40–0-mb-layer zonal generations of this report lie halfway

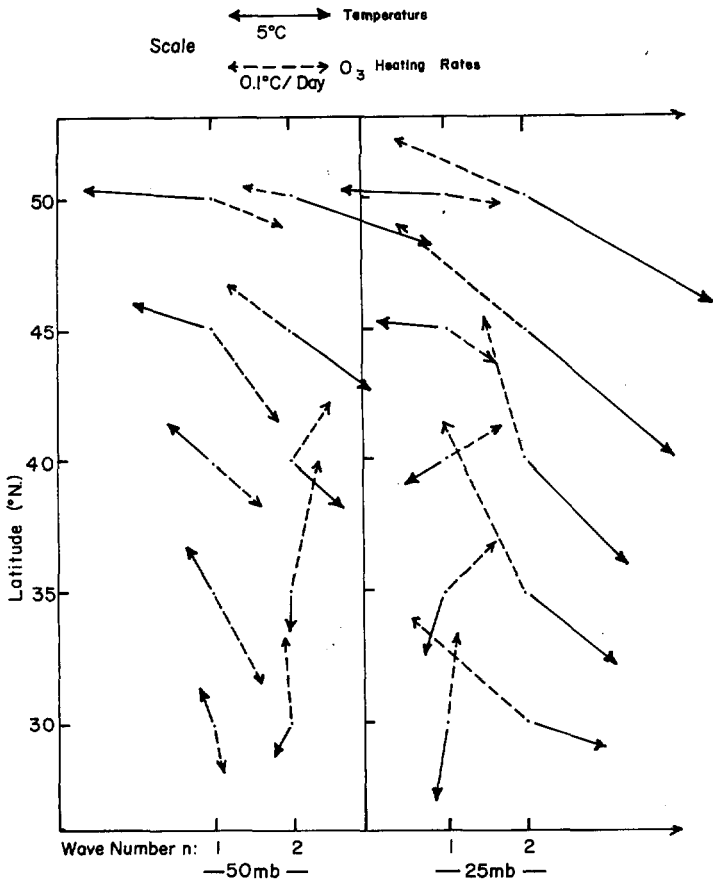

FIGURE 7.—Latitudinal distribution of the amplitudes and phases of the 25-mb and 50-mb wave numbers 1 and 2 temperature and heating rates. The heating rates are due to the absorption by ozone in the 9.6-micron band. The length of each vector is proportional to the amplitude of its corresponding Fourier wave while the vector direction indicates its phase location. The scale attached refers to the magnitudes of the vector components. The results are valid for Jan. 12, 1959.

between those of Perry (1966) and Kennedy (1964). The eddy generation values (*GE*) agree generally well with the few cases listed. Some comments are given with respect to Perry's results for the 40–0-mb layer. His mean value of -3.73 ergs cm^{-2} mb^{-1} sec^{-1} comes from a very variable set of values (standard deviation of 6.81 ergs cm^{-2} mb^{-1} sec^{-1}). Much of this daily variability disappears when the eddy generation is integrated over the whole stratosphere. This would tend to show that both the numerical error randomness of Perry's dynamically inferred eddy generations and the interlevel radiative interactions act in such a way as to decrease the noise level when integrated over the whole stratosphere. It is thought that our eddy generation values are smaller than they should be since they were not found sufficiently large to balance the budget of the eddy potential energy reservoir (Paulin, 1968).

5. CONCLUSION

A method of computing the stratospheric heating rates from daily available data of the Northern Hemisphere has been given. It consists of a hybrid approach using both simple parametric relations (solar ultraviolet absorption)

TABLE 7.—*Comparison of generation of available potential energy with various investigators (units: ergs cm^{-2} mb^{-1} sec^{-1})*

Source	Period	Layer (mb)	*GZ*	*GE*
Paulin	Jan. 12–16, 1959	25	0.29	−0.74
Paulin	do.	40–0	0.80	−1.13
Paulin	do.	150–0	0.04	−0.89
Perry (1966)	Jan. 2–19, 1963	40–0	1.06	−3.73
Perry (1966)	do.	200–0	−0.37	−1.45
Julian and Labitzke (1965)	Jan. 2–27, 1963	100–10	−1.59	−0.36
Kennedy (1964)	Jan. (mean)	40–10	0.61	
Kennedy (1964)	do.	200–10	−0.82	
Muench (1965)	Jan. 1958	100–10	0.36	
Oort (1963)	Oct.–Dec. 1957	100–30	−0.45	

and full radiative transfer calculations in the long-wave spectrum (absorption in the 15-micron band of carbon dioxide and in the 9.6-micron band of ozone). The ultraviolet solar absorption has only latitudinal and time variations. The 15-micron CO_2 cooling has latitudinal, longitudinal, and time variations, being a function of temperature. The 9.6-micron ozone absorption was also hybrid, since it used the complete temperature field and only latitudinal variations of the vertical ozone profiles averaged for the month. The resulting total heating rates were found to be realistic. The tropospheric large-scale cloud distribution was found to affect the stratospheric total cooling rates by decreasing the heating due to the 9.6-micron band of ozone.

This method has been applied in the stratosphere for the period Jan. 12 to 16, 1959, in order to compute the generation of available potential energy. The results agreed generally well with other studies. However, the eddy generations yielded negative values of smaller magnitudes than would be required to balance the eddy available potential energy budget and also generally smaller values than those from other studies. This anomaly was probably due to incomplete specification in the solar ultraviolet and 9.6-micron ozone absorption and in the carbon dioxide cooling (a somewhat smoother vertical temperature field than found in the atmosphere).

Some interlevel radiative interactions have been observed and diagnosed. The generation of eddy available energy was found to be more negative at 50 mb than at 25 mb, this being especially reflected in the scale of wave number 1. This is due to radiative transfers between nearby atmospheric layers associated with varying lapse rates. The tropospheric-stratospheric radiative interaction through the 9.6-micron band of ozone has been clarified. There is a systematic destruction of eddy available energy in stratospheric wave numbers 1 and 2, the effect being maximum at or near 50 mb, through the radiative coupling between large-scale dynamically controlled features of the troposphere.

It is concluded that because of the directness and the easy access to daily data characterizing this radiative

computation method, one could use it with profit to evaluate daily stratospheric heating functions. The usefulness of the method is indicated, as it yielded reasonable generations of available potential energy in the stratosphere.

ACKNOWLEDGMENTS

The author wishes to thank Prof. B. W. Boville for providing him the opportunity to investigate the problem treated here, Dr. P. E. Merilees for critically reviewing the original manuscripts and suggesting many improvements, and the Meteorological Service of Canada for the approval of this publication.

REFERENCES

Bojkov, R. D., "The Vertical Ozone Distribution in the Earth Atmosphere," *Meteorologiia i Gidrologiia*, No. 10, Moskskoe Otdelenie Gidrometeoizdata, Moscow, Oct. **1965**, pp. 3–11.

Bojkov, R. D., "Differences in the Vertical Ozone Distribution Deduced From Umkehr and Ozonesonde Data at Goose Bay," *Journal of Applied Meteorology*, Vol. 5, No. 6, Dec. **1966**, pp. 872–877.

Brown, J. A., Jr., "A Disgnostic Study of Tropospheric Diabatic Heating and the Generation of Available Potential Energy," *Tellus*, Vol. 16, No. 3, Aug. **1964**, pp. 371–388.

Burch, D. E., Gryvnak, D., Singleton, E. B., France, W. L., and Williams, D., "Infrared Absorption by Carbon Dioxide, Water Vapour and Minor Atmospheric Constituents," *Research Report*, Contract No. AF19(604)–2633, Ohio State University, Columbus, July **1962**, 316 pp.

Clark, J. H., "Infrared Heating Due to Ozone," M.S. thesis, Department of Meteorology, McGill University, Montreal, Quebec, **1963**, 52 pp.

Davis, P. A., "A Re-Examination of the Heat Budget of the Troposphere and Lower Stratosphere," *Scientific Report* No. 3, Contract No. AF19(604)–6146, Research Division, College of Engineering, New York University, Oct. **1961**, 115 pp.

Davis, P. A., "An Analysis of the Atmospheric Heat Budget," *Journal of the Atmospheric Sciences*, Vol. 20, No. 1, Jan. **1963**, pp. 5–22.

Dutsch, H. U., *Uniform Evaluation of Umkehr Observation from World Ozone Network: Part III. World Wide Ozone Distribution at Different Levels and Its Variation with Season from Umkehr Observations*, National Center for Atmospheric Research, Boulder, Colo., Dec. **1964**, 34 pp.

Hering, W. S., and Borden, T. R., Jr., "Mean Distributions of Ozone Density Over North America 1963–1964," *Environmental Research Papers* No. 162, Air Force Cambridge Research Laboratories, Hanscom Field, Mass., Dec. **1965**, 19 pp.

Hering, W. S., Touart, C. N., and Borden, T. R., Jr., "Ozone Heating and Radiative Equilibrium in the Lower Stratosphere," *Journal of the Atmospheric Sciences*, Vol. 24, No. 4, July **1967**, pp. 402–413.

Houghton, J. T., "The Absorption of Solar Infra-Red Radiation by the Lower Stratosphere," *Quarterly Journal of the Royal Meteorological Society*, Vol. 89, No. 381, July **1963**, pp. 319–331.

Julian, P. R., and Labitzke, K. B., "A Study of Atmospheric Energetics During the January–February 1963 Stratospheric Warming," *Journal of the Atmospheric Sciences*, Vol. 22, No. 6, Nov. **1965**, pp. 597–610.

Kennedy, J. S., "Energy Generation Through Radiative Processes in the Lower Stratosphere," *Report* No. 11, Contract No. AT(30–1)2241, Department of Meteorology, Massachusetts Institute of Technology, Cambridge, Dec. **1964**, 116 pp.

Kriester, B., Labitzke-Behr, K., Petkovšek, Z., Scherhag, R., Stuhrmann, R., and Warnecke, G., "Tägliche Höhenkarten der 50-mbar-Fläche sowie monatliche Mittelkarten für das Jahr 1959. Teil I. 1. Vierteljahr," (Daily Upper Air Charts for the 50-Millibar Surface as well as Monthly Mean Charts for 1959, Part 1, First Quarter), *Meteorologische Abhandlungen*, Band XXIX, Heft 1, Institut für Meteorologie und Geophysik der Freien Universität Berlin, Verlag Von Dietrich Reimer, Berlin, **1962.**

Labitzke-Behr, K., Petkovšek, Z., Scherhag, R., and Warnecke, G., "Tägliche Höhenkarten der 10-mbar-Fläche sowie monatliche Mittelkarten für das Jahr 1959. Teil I. 1. Vierteljahr," (Daily Upper Air Charts for the 10-Millibar Surface as well as Monthly Mean Charts for 1959. Part 1. First Quarter), *Meteorologische Abhandlungen*, Band XXXI, Heft 1, Institut für Meteorologie und Geophysik der Freien Universität Berlin, Verlag Von Dietrich Reimer, Berlin, **1962.**

Lorenz, E. N., "Available Potential Energy and the Maintenance of the General Circulation," *Tellus*, Vol. 7, No. 2, May **1955**, pp. 157–167.

Mateer, C. L., "A Study of the Information Content of Umkehr Observations," *Technical Report* No. 2, National Science Foundation Grant No. G–19131, Department of Meteorology and Oceanography, University of Michigan, Ann Arbor, Apr. **1964**, 199 pp.

Muench, H. S., "Stratospheric Energy Processes and Associated Atmospheric Long-Wave Structure in Winter," *Environmental Research Papers* No. 95, U.S. Air Force, Cambridge Research Laboratories, Hanscom Field, Mass., Apr. **1965**, 120 pp.

Ohring, G., "The Radiation Budget of the Stratosphere," *Journal of Meteorology*, Vol. 15, No. 5, Oct. **1958**, pp. 440–451.

Oort, A. H., "On the Energy Cycle in the Lower Stratosphere," *Report* No. 9, Contract No. AT(30–1)2241 and AF19(604)–5223, Department of Meteorology, Massachusetts Institute of Technology, Cambridge, Dec. 15, **1963**, 122 pp.

Paulin, G., "Stratospheric Heating Rates," *Arctic Meteorology Research Group Publication in Meteorology* No. 81, McGill University, Montreal, Quebec, **1966**, 98 pp.

Paulin, G., "Spectral Atmospheric Energetics During January 1959," *Arctic Meteorology Research Group Publication in Meteorology* No. 91, McGill University, Montreal, Quebec, June **1968**, 328 pp.

Perry, J. S., "The Energy Balance of the Atmosphere During a Sudden Stratospheric Warning," Ph. D. thesis, University of Washington, Seattle, **1966**, 185 pp.

Rodgers, C. D., and Walshaw, C. D., "The Computation of Infrared Cooling Rate in Planetary Atmospheres," *Quarterly Journal of the Royal Meteorological Society*, Vol. 92, No. 391, Jan. **1966**, pp. 67–92.

Walshaw, C. D., "Integrated Absorption by the 9.6μ Band of Ozone," *Quarterly Journal of the Royal Meteorological Society*, Vol. 83, No. 357, July **1957**, pp. 315–321.

Wiin-Nielsen, A., "On Energy Conversion Calculations," *Monthly Weather Review*, Vol. 92, No. 4, Apr. **1964**, pp. 161–167.

[Received August 20, 1968; revised September 30, 1968]